

RECOMMENDATION ITU-R P.1817*

Propagation data required for the design of terrestrial free-space optical links

(Question ITU-R 228/3)

(2007)

Scope

This Recommendation provides propagation data required for the design of free-space optical (FSO) links and planning of free-space optical systems, in the respective ranges of validity indicated in the Recommendation.

The ITU Radiocommunication Assembly,

considering

- a) that the visible optical and infrared spectrum is available for radiocommunications in the Earth's environments;
- b) that for the proper planning of free-space optic (FSO) radiocommunication systems operating in visible optical and infrared spectrum, it is necessary to have appropriate propagation data;
- c) that methods have been developed that allow the calculation of the most important propagation parameters needed in planning free-space optical systems operating in visible optical and infrared spectrum;
- d) that, as far as possible, these methods have been tested against available data and have been shown to yield an accuracy that is both compatible with the natural variability of propagation phenomena and adequate for most present applications in the planning of systems operating in the visible optical and infrared spectrum,

recognizing

- a) that No. 78 of Article 12 of the ITU Constitution states that a function of the Radiocommunication Sector includes, "... carrying out studies without limit of frequency range and adopting recommendations ...",

recommends

- 1** that the methods for predicting the propagation parameters given in Annex 1 should be adopted for planning free-space optical systems, in the respective ranges of validity indicated in the Annex.

NOTE 1 – Supplementary information related to propagation prediction methods for frequencies in visible and infrared spectrum may be found in an ITU-R Recommendation on prediction methods required for the design of terrestrial free-space optical links.

* This Recommendation should be brought to the attention of Radiocommunication Study Groups 1 and 9.

Annex 1

1 Atmospheric considerations

FSO links are impaired by absorption and scattering of light by the Earth's atmosphere. The atmosphere interacts with light due to the composition of the atmosphere, which normally consists of a variety of different molecular species and small suspended particles called aerosols. This interaction produces a wide variety of phenomena: frequency selective absorption, scattering, and scintillation.

- Frequency selective absorption at specific optical wavelengths results from the interaction between the photons and atoms or molecules that leads to the extinction of the incident photons, elevation of the temperature, and radiative emission.
- Atmospheric scattering results from the interaction between the photons and the atoms and molecules in the propagation medium. Scattering causes an angular redistribution of the radiation with or without modification of the wavelength.
- Scintillation results from thermal turbulence within the propagation medium that results in randomly distributed cells. These cells have variable sizes (10 cm-1 km), temperatures, and refractive indices causing scattering, multipath and variation of the angles of arrival. As a result, the received signal amplitude fluctuates at frequencies ranging between 0.01 and 200 Hz. Scintillation also causes wave front distortion resulting in defocusing of the beam.

In addition, sunlight can affect FSO performance when the sun is co-linear with the direction of the free-space optical link.

2 Molecular absorption

Molecular absorption results from an interaction between the optical radiation and the atoms and molecules of the medium (N₂, O₂, H₂, H₂O, CO₂, O₃, Ar, etc.). The absorption coefficient depends on the type and concentration of gas molecules. The spectral variations of the absorption coefficient determine the absorption spectrum. The nature of this spectrum is due to the variations of possible energy levels of the gas generated essentially by the electronic transitions, vibrations of the atoms, and rotation of the molecules. An increase in the pressure or temperature tends to widen the spectral absorption lines by excitation of higher energy levels and by the Doppler effect. Molecular absorption is a selective phenomenon that results in relatively transparent atmospheric transmission windows, and relatively opaque atmospheric absorption bands.

The transmission windows in the optical range are:

- Visible and very-near IR: from 0.4 to 1.4 μm
- Near IR or IR I: from 1.4 to 1.9 μm and 1.9 to 2.7 μm
- Mean IR or IR II: from 2.7 to 4.3 μm and 4.5 to 5.2 μm
- Far IR or IR III: from 8 to 14 μm
- Extreme IR or IR IV: from 16 to 28 μm.

The gaseous molecules have quantified energy levels proper to each species, and can absorb energy (or photons) under the influence of an incident electromagnetic radiation and transition from an initial energy level, e_i , to a higher energy level, e_f . The radiation energy is then attenuated by the loss of one or more photons.

This process only occurs if the incident wave frequency corresponds exactly to one of the resonance frequencies of the considered molecule, given by:

$$\nu_0 = \frac{e_f - e_i}{h} \tag{1}$$

where:

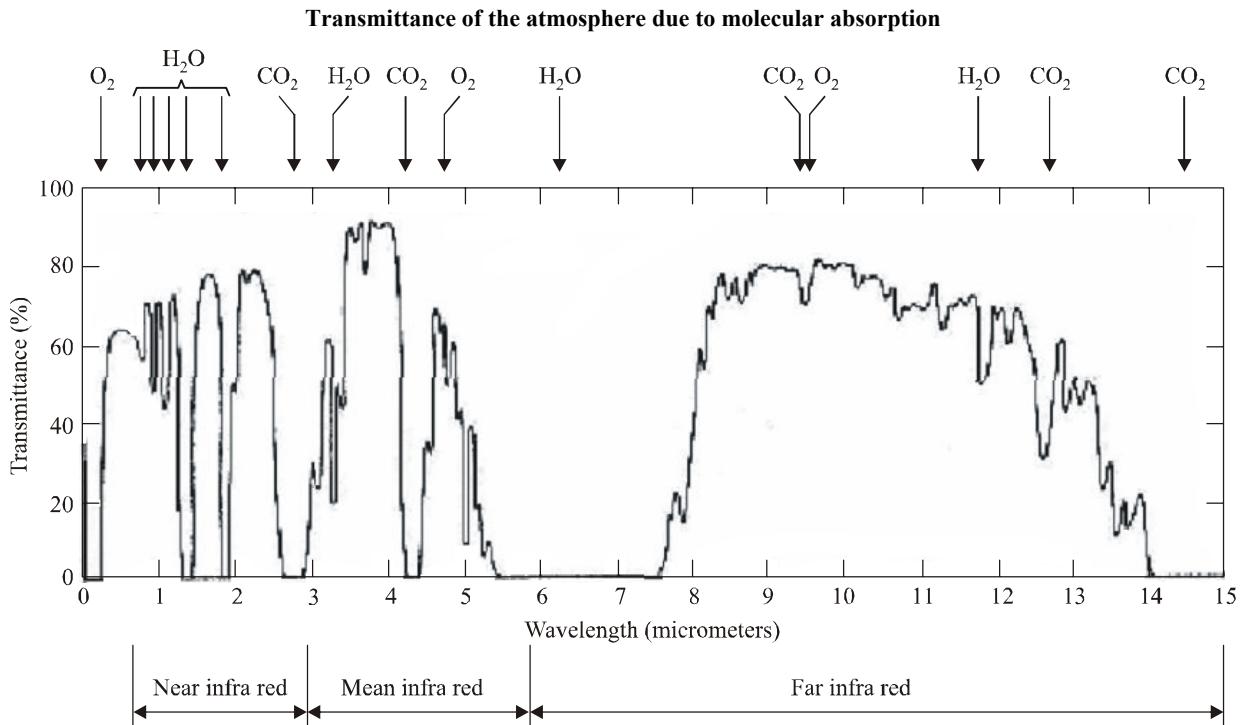
ν_0 : incident wave frequency (Hz)

h : Planck's constant, $h = 6.6262 \cdot 10^{-34}$ J-s.

The fundamental parameters that determine the absorption generated by molecular resonance are: the possible energy levels for each molecular species the probability of transition from an energy level e_i to an energy level e_f , the intensity of resonance lines, and the natural profile of each line.

Generally, the profile of each absorption line is modified by the Doppler effect when the molecules are moving relative to the incident wave, and by the collision effect due to the interaction of the molecules. These phenomena lead to a spectral widening of the natural line of each molecule. For certain molecules, such as in carbon dioxide (CO₂), water vapour (H₂O), nitrogen (N₂) and oxygen (O₂), the absorption line profiles can extend sufficiently far from each central line. This property leads to an absorption continuum. Figure 1 shows the nominal measured atmosphere transmittance due to molecular absorption on a 1 820 m horizontal link at sea level.

FIGURE 1



1817-01

3 Molecular scattering

Molecular scattering results from the interaction of light with atmospheric particles whose sizes are smaller than the wavelength of the incident light. Scattering by atmospheric gas molecules (Rayleigh scattering) contributes to the total attenuation of the electromagnetic radiation.

The extinction coefficient due to molecular scattering, $\beta_m(\lambda)$, is:

$$\beta_m(\lambda) = \frac{24\pi^3}{\rho\lambda^4} 10^3 \left(\frac{[n(\lambda)]^2 - 1}{[n(\lambda)]^2 + 2} \right) \left(\frac{6 + 3\delta}{6 - 7\delta} \right) \quad (2)$$

where:

- $\beta_m(\lambda)$: molecular scattering coefficient (km^{-1})
- λ : wavelength (μm)
- ρ : molecular density (m^{-3})
- δ : depolarization factor of the air ($\cong 0.03$)
- $n(\lambda)$: refractive index of air.

An approximate value of $\beta_m(\lambda)$ is:

$$\beta_m(\lambda) = A\lambda^{-4} \quad (3)$$

where:

$$A = 1.09 * 10^{-3} \frac{P}{P_0} \frac{T_0}{T} \quad \text{km}^{-1} \text{m}^4 \quad (4)$$

and

- P : atmospheric pressure (mbar)
- P_0 : 1 013 mbar
- T : atmospheric temperature (K), and
- T_0 : 273.15 K.

Molecular scattering is negligible at infrared wavelengths, and Rayleigh scattering primarily affects ultraviolet wavelengths up to visible wavelengths. The blue colour of the clear-sky background is due to this type of scattering.

4 Aerosol absorption

Aerosols are extremely fine solids or liquids particles suspended in the atmosphere with very low fall speed (ice, dust, smoke, etc). Their size generally lies between 10^{-2} and $100 \mu\text{m}$. Fog, dust and maritime spindrift particles are examples of aerosols.

Aerosols influence the conditions of atmospheric attenuation due to their chemical nature, their size and their concentration. In maritime environments, the aerosols are primarily made up of droplets of water (foam, fog, drizzle, rain), salt crystals, and various particles of continental origin. The type and density of continental particles depend on the distance from, and characteristics of, the neighbouring coasts.

The extinction coefficient due to aerosol absorption, $\alpha_n(\lambda)$, is:

$$\alpha_n(\lambda) = 10^5 \int_0^{\infty} Q_a \left(\frac{2\pi r}{\lambda}, n'' \right) \pi r^2 \frac{dN(r)}{dr} dr \quad \text{km}^{-1} \quad (5)$$

where:

- λ : wavelength (μm)
- $dN(r)/dr$: particle size distribution per unit of volume (cm^{-4})

n'' : imaginary part of the refractive index, n , of the considered aerosol

r : radius of the particles (cm)

$Q_a(2\pi r/\lambda, n'')$: absorption cross-section for a given type of aerosol.

Mie theory predicts the electromagnetic field diffracted by homogeneous spherical particles. The absorption (Q_a) and scattering (Q_d) cross-sections depend on the particle size, refractive index and incident wavelength. They represent the portion of an incident wave where the absorbed (scattered) power is equal to the incident power.

The refractive index of aerosols depends on their chemical composition and the wavelength. It is denoted as $n = n' + n''$ where n' is a function of the scattering capacity of the particle, and n'' is a function of the absorption of the particle.

In the visible and near infrared spectral regions, the imaginary part of the refractive index is extremely low and can be neglected in the calculation of global attenuation (extinction). In the far infrared case, the imaginary part of the refractive index must be taken into account.

5 Aerosol scattering

Aerosol scattering (Mie scattering) occurs when the particle size is the same order of magnitude as the wavelength of the incident light. Attenuation is a function of frequency and visibility, and visibility is related to the particle size distribution. This phenomenon constitutes the most restrictive factor to the deployment of free-space optical systems at long distances. In the optical region, it is mainly caused by mist and fog. The attenuation in the optical regime can reach 300 dB/km, in contrast to the millimetre wave region, where rain attenuation is typically a few dB/km.

The extinction coefficient due to aerosol scattering, β_n , is given by the following relation:

$$\beta_n(\lambda) = 10^5 \int_0^{\infty} Q_d\left(\frac{2\pi r}{\lambda}, n'\right) \pi r^2 \frac{dN(r)}{dr} dr \quad \text{km}^{-1} \quad (6)$$

where:

λ : wavelength (μm)

$dN(r)/dr$: particle size distribution per unit of volume (cm^{-4})

n' : real part of the refractive index n of the aerosol

r : radius of the particles (cm)

$Q_d(2\pi r/\lambda, n')$: scattering cross-section for a given type of aerosol.

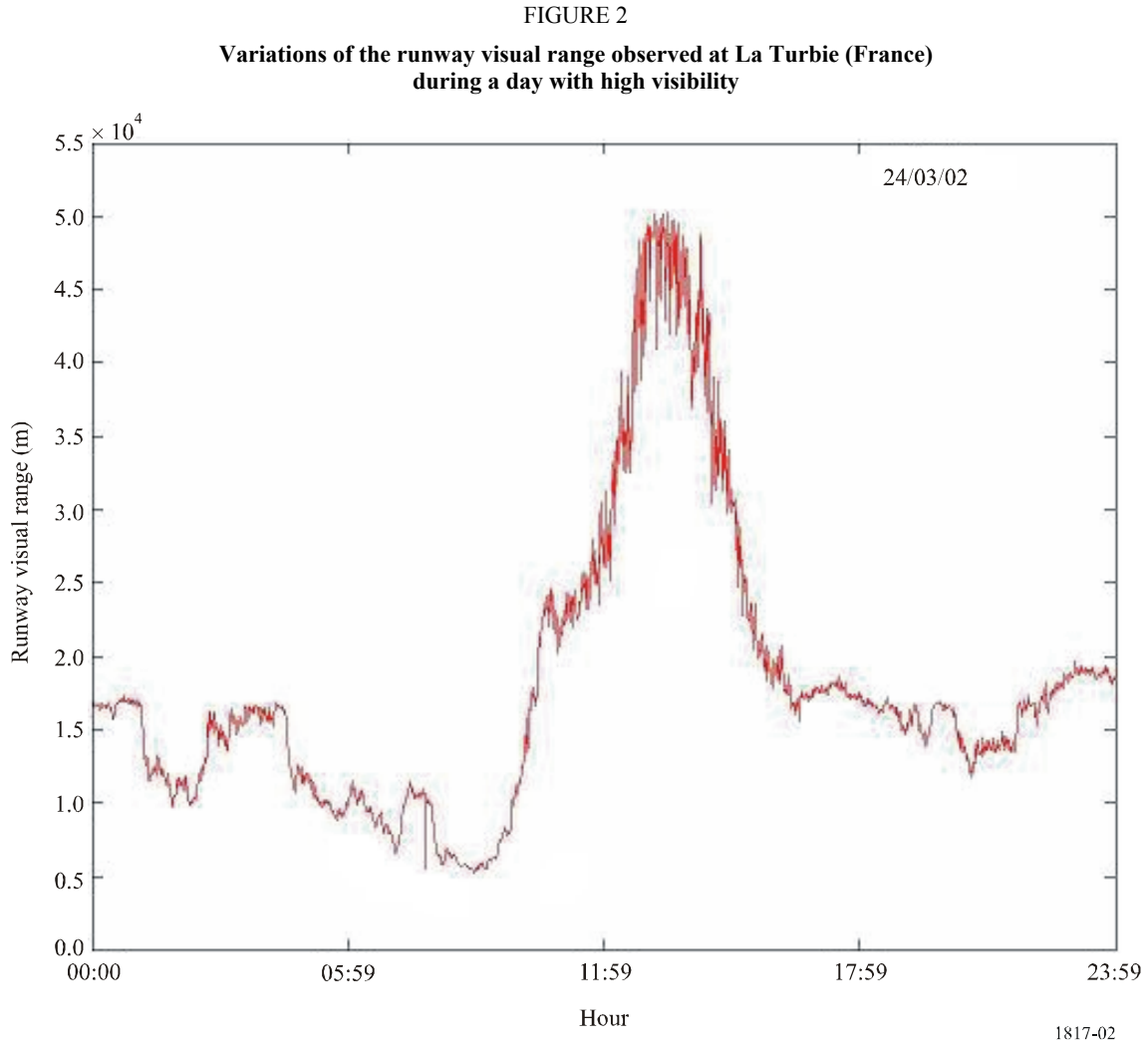
Mie theory predicts the scattering coefficient Q_d due to the aerosols, assuming the particles are spherical and sufficiently separated so that the scattered field can be calculated assuming far field (single) scattering.

The scattering cross-section Q_d strongly depends on the size of the aerosol compared to the wavelength, and is a very frequency-selective function for particles whose radius is less than or equal to the wavelength. It reaches its maximum value (3.8) for a particle radius equal to the wavelength, in which case the scattering is maximal. As the size of the particle increases, the scattering cross-section asymptotes to a value approximately equal to 2.

Since the aerosol concentration, composition and size distribution vary temporally and spatially, it is difficult to predict attenuation by these aerosols. Although the concentration is closely related to the optical visibility, there is not a unique particle size distribution for a given visibility.

Visibility characterizes the transparency of the atmosphere as estimated by a human observer. It is measured by the runway visual range (RVR), and is the distance that a luminous beam must travel through the atmosphere for its intensity (or luminous flux) to drop to 0.05 times its original value. It may be measured using a transmissometer or a diffusiometer.

Figure 2 gives an example of the variations of the runway visual range observed at La Turbie, France, during a day with high visibility.



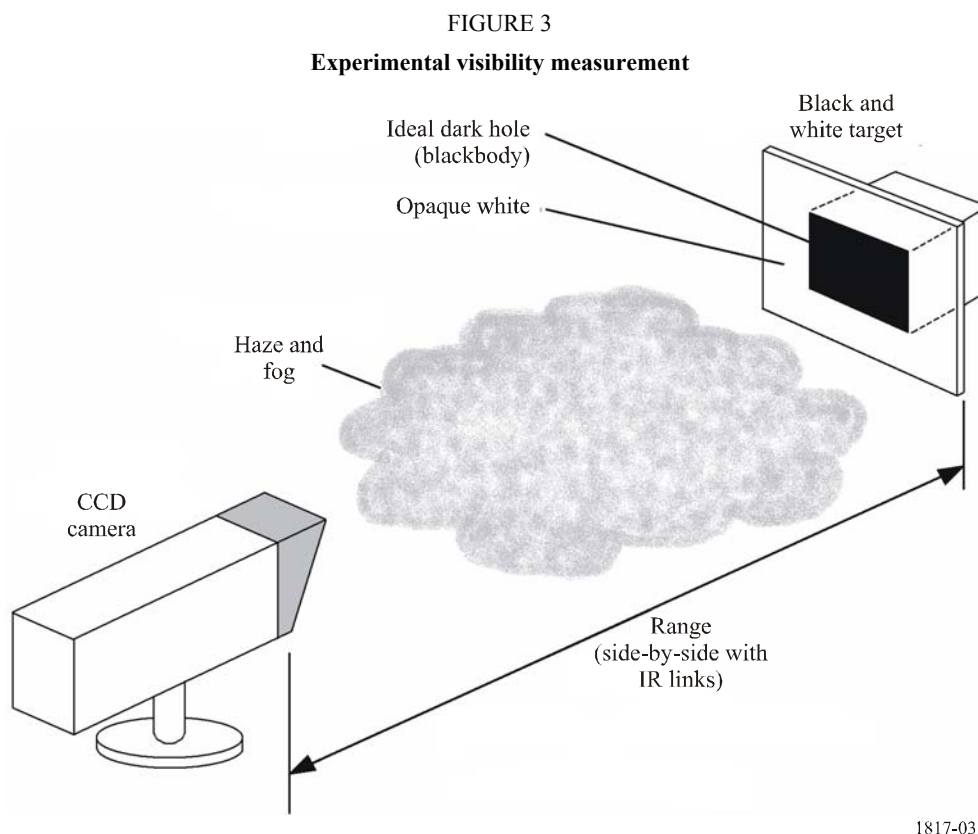
Alternatively, visibility along the transmission path can be measured using a CCD camera and a black and white reference target. For this method, the visual range, V_r , is given by:

$$V_r = \frac{\ln(0.02)}{\ln(C/C_0)} d \quad (7)$$

C is the measured contrast between the black and white regions of the target, C_0 is the intrinsic contrast ratio of the target (measured close to it), and d is the distance to the target. The value of C is given by the relation:

$$C = \frac{L_w - L_b}{L_w + L_b} = 0.02 = e^{-b_{EX} \cdot V_r} \quad (8)$$

where L_w and L_b are the luminance of the white and black parts of the target, b_{EX} is the extinction coefficient and V_r the visual range. Figure 3 shows the ideal target, with the black part of the target the surface of a cavity in a white painted panel, and the inside surface of the hole painted black to avoid any directly scattered light.



All the optical characteristics of aerosols, and in particular, fog, are related to the particle size distribution which may be regarded as the key parameter to determine physical and optical properties of fog.

Generally this distribution is represented by analytical functions such as the lognormal distribution for aerosols and the modified gamma distribution for fog. The latter is largely used to model the various types of fog and clouds, and is given by:

$$N(r) = ar^{\alpha} \exp(-br) \quad (9)$$

where $N(r)$ is the number of particles per unit volume and per unit increment of the radius r , and α , a and b are parameters that characterize the particle size distribution.

Computer codes (see Appendix 1 to Annex 1) usually take into account two particular cases: heavy advection fog and moderate radiation fog, which are modelled by the modified gamma size distribution as shown above. Typical parameters of the modified gamma distribution are given in Table 1.

TABLE 1

**Various parameters of the particles size distribution for a dense advection fog
and a moderate radiation fog**

	α	a	b	N (cm ⁻³)	W (g/m ³)	r_m (μm)	V (m)
Heavy advection fog	3	0.027	0.3	20	0.37	10	130
Moderate radiation fog	6	607.5	3	200	0.02	2	450

where:

- N : total number of water particles per unit volume (cm³)
- r_m : modal radius (μm) for which the distribution presents a maximum
- W : liquid water content (g/m³)
- V : visibility associated to the fog type (m).

The received signal level can experience significant short-term fluctuations due to variations in visibility. Figure 4 shows the normalized received intensities of far IR and mid IR links, together with the link visibility during a minute slot.

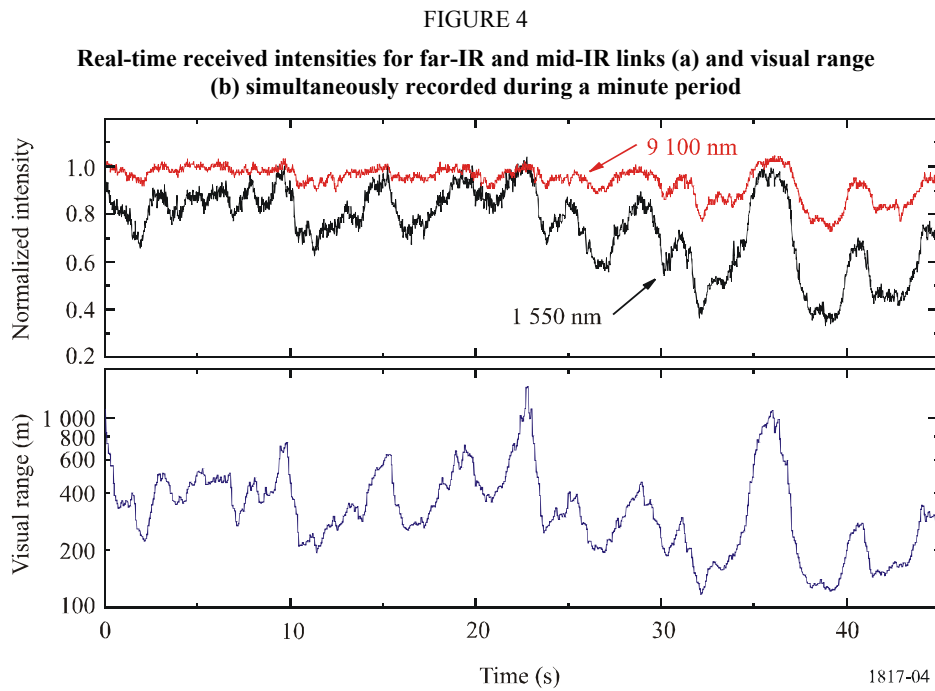
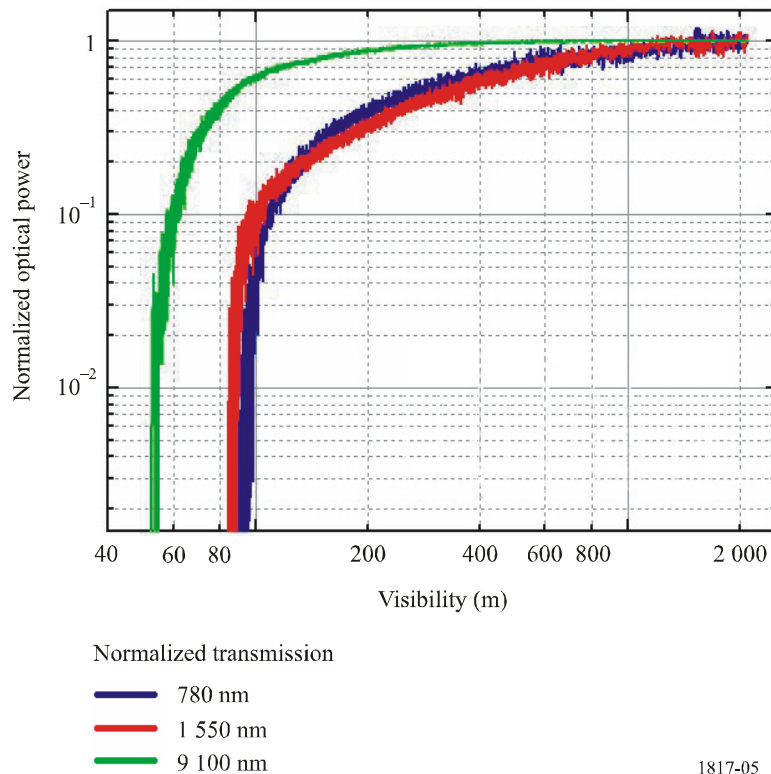


Figure 5 shows normalized optical power as a function of the visual range, measured at 780 nm, 1 550 nm and 9 100 nm.

FIGURE 5

Normalized received optical power versus link visibility for three different wavelengths



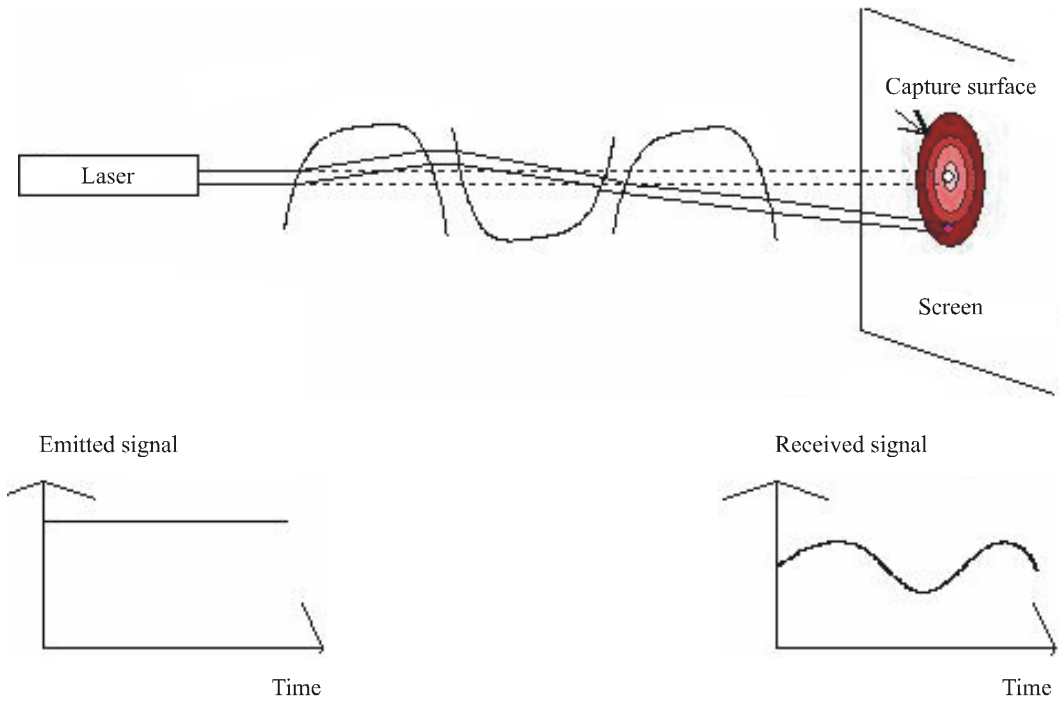
In many cases of thick fog, the particle distribution is non uniform. In this case, far-IR links could provide superior availability, because 10 μm light can overcome losses in dense fog and maintain link availability whereas shorter wavelength light can not.

6 Scintillation

Randomly distributed cells of varying refractive index can be formed within the propagation medium under the influence of thermal turbulence. These cells cause scattering, multipath, and variation in the angle of arrival, causing the received signal level to fluctuate at frequencies between 0.01 and 200 Hz. Wave front variations similarly cause time-varying focusing and defocusing of the beam. Such fluctuations of the signal are called scintillation. The amplitude and the frequency of scintillation depend on the size of the cells compared to the diameter of the beam. The following figures show this effect as well as the variations (amplitude, frequency) of the received signal. The beam deviates (Fig. 6) when heterogeneities are large compared to the beam cross-section, and the beam is widened (Fig. 7) when heterogeneities are small compared to the beam cross-section. A mixture of heterogeneities results in scintillation (Fig. 8).

FIGURE 6

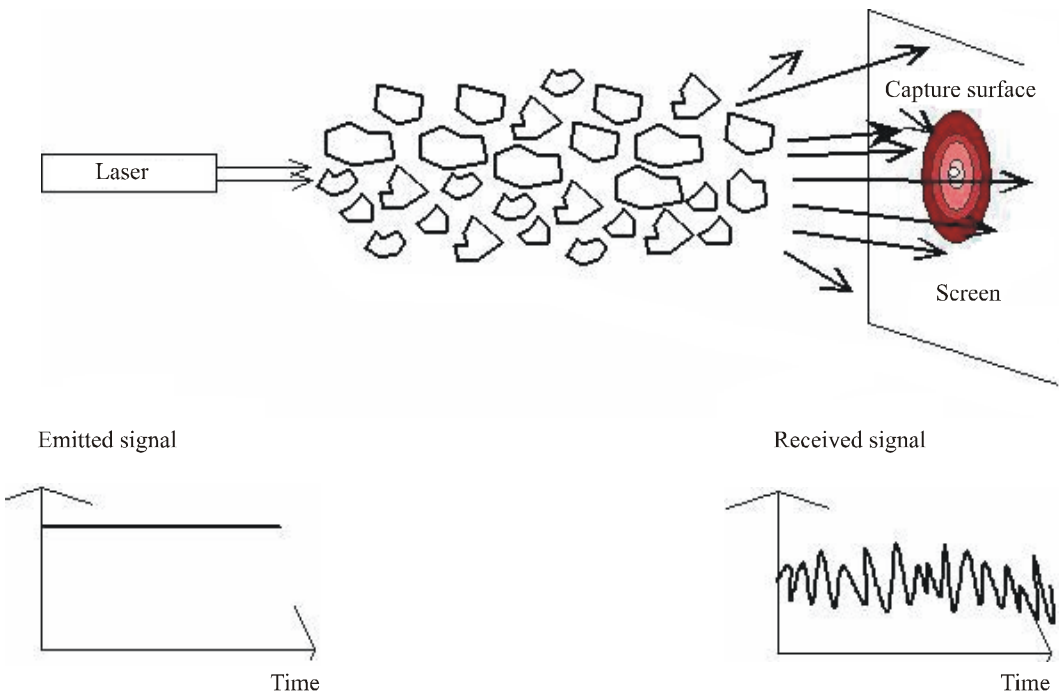
Deviation of the beam under the influence of turbulent cells larger than the beam diameter



1817-06

FIGURE 7

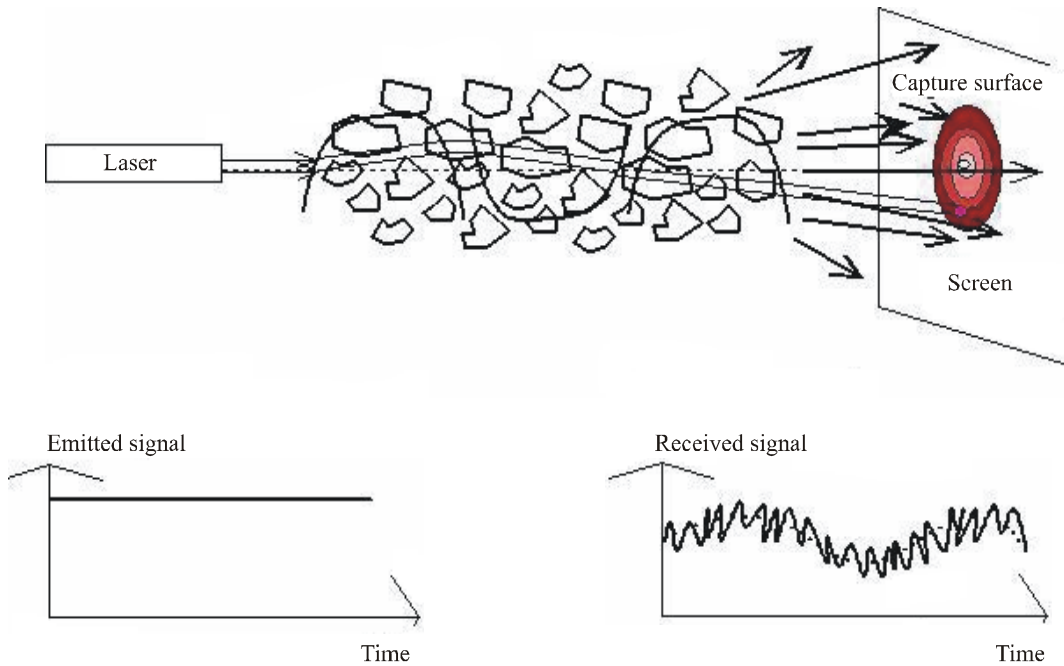
Deviation of the beam under the influence of turbulent cells smaller than the beam diameter (widening of the beam)



1817-07

FIGURE 8

Effects of different size heterogeneities on laser beam propagation (scintillation)



1817-08

7 Rain attenuation

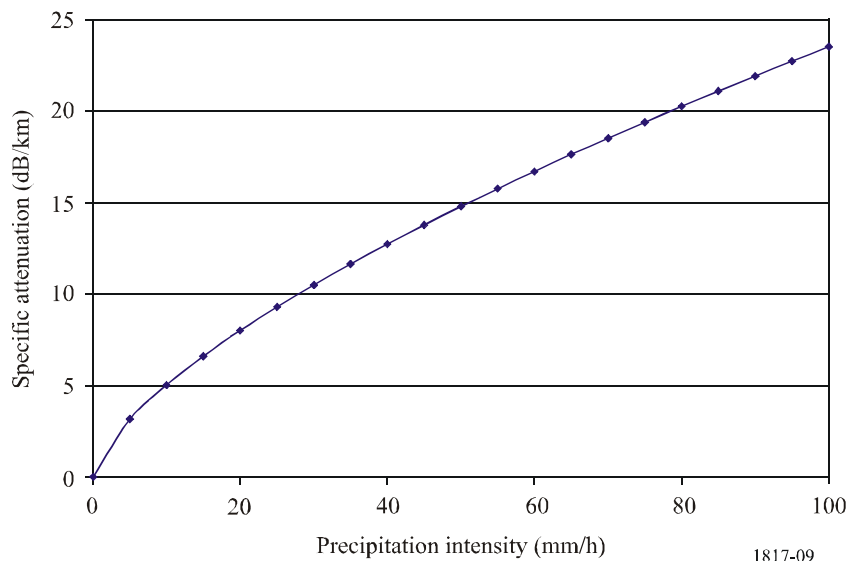
Specific attenuation (dB/km) due to rain is generally approximated by the relation:

$$\gamma_{rain} = k \cdot R^\alpha \tag{10}$$

Figure 9 illustrates typical variations of the specific attenuation (dB/km) due to precipitation observed in the optical and infrared ranges.

FIGURE 9

Specific attenuation (dB/km) due to precipitation in optical and infrared ranges



1817-09

Recommendation ITU-R P.837 gives the rainfall rate, R_p (mm/h), exceeded for a given percentage of the average year, p , and for any location.

8 Snow attenuation

Specific attenuation (dB/km) due to snow as a function of snowfall rate is given by the following relation:

$$\gamma_{snow} = a \cdot S^b \quad (11)$$

where:

- γ_{snow} : specific attenuation (dB/km) due to snow
- S : snowfall rate (mm/h)
- a and b : functions of wavelength, λ (nm), and are given in Table 2:

TABLE 2
Parameters “ a ” and “ b ” for wet and dry snow

	a	b
Wet snow	$0.0001023\lambda_{nm} + 3.7855466$	0.72
Dry snow	$0.0000542\lambda_{nm} + 5.4958776$	1.38

The estimated attenuation as a function of snowfall rate for $\lambda = 1.55 \mu\text{m}$ is shown in Figs. 10 and 11.

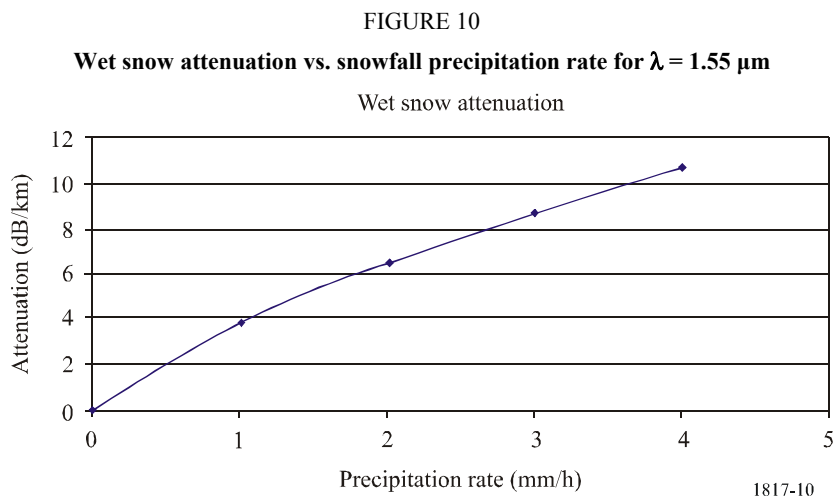
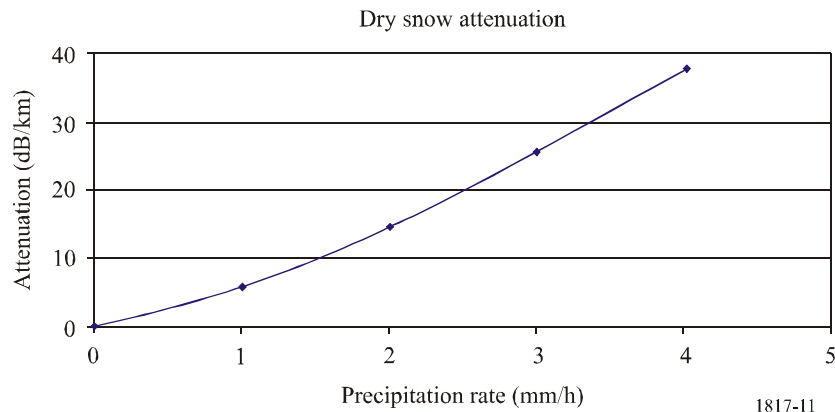


FIGURE 11
 Dry snow attenuation vs. snowfall precipitation rate for $\lambda = 1.55 \mu\text{m}$



9 Ambient light effect

Solar conjunction occurs when the sun or a reflected image of the sun is in or near the instantaneous field of view (IFOV) of an optical receiver. The receive IFOV is generally at least as large as the transmit divergence. The aim is to calculate the probability for which the sun position is parallel to the optical link, and the sun power penetrating inside the receiver is greater than the power received from the emitter. A method to estimate this effect is found in Recommendation ITU-R P.1814.

10 Cumulative distribution of attenuation

Cumulative distributions of attenuation measured at 850 nm on a 850 m path due to: all hydrometeors, fog, rain, rain + snow, and snow in Prague, Czech Republic, during a 1-year period are shown in Fig. 12. All fading events were classified according to the meteorological conditions causing a particular fade event. The meteorological conditions were identified using a camera image of the area between the transmitter and the receiver and using data obtained from an automatic meteorological station located near the receiver. Fading events caused by fog and by snow were the most serious.

11 Hybrid/FSO systems

Figure 13 compares attenuation measurements at 58 GHz and an optical link on the same path due to all hydrometeors and rain only. The optical path had less attenuation than the millimetre wave path during rain events. Hybrid radio/optical (RF/FSO) systems can improve FSO link performance by taking advantage of the fact that an RF path is attenuated by rain but insensitive to fog. In contrast, an optical path is heavily attenuated by fog and is relatively insensitive to rain.

Annual cumulative distributions depicted in Fig. 13 give an estimation of the performance of a hypothetical hybrid RF/FSO system. Consider a hybrid system where the RF and optical paths have the same fade margin, $FM = 20$ dB. A simple diversity technique is used, so either the RF or FSO part of the system is active depending on the instantaneous values of the RF and optical path attenuation. It is assumed that the RF part of the system mitigates non-rain events, and the FSO part mitigates rain events. The availability ratio (AR) of the hybrid system is estimated from the FSO rain statistics as shown in Table 3.

FIGURE 12

Cumulative attenuation distributions for different path conditions

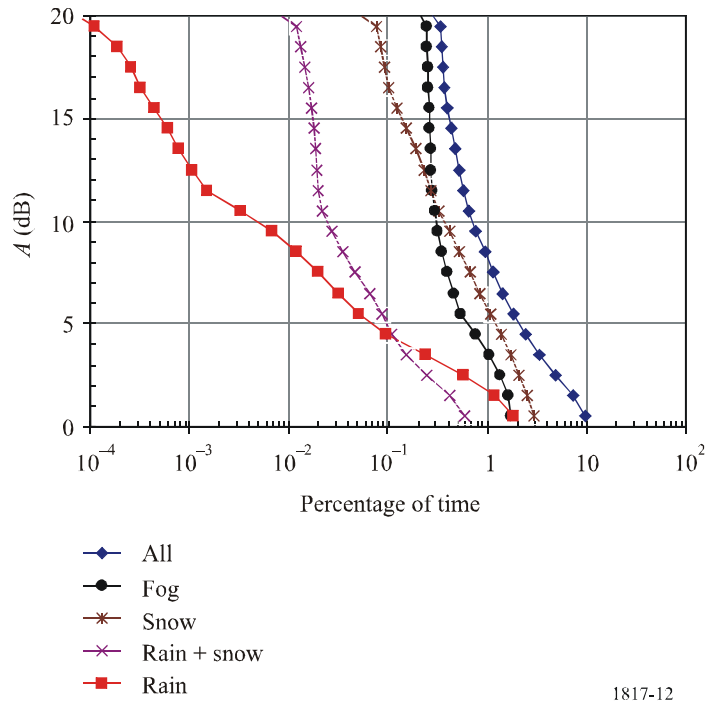


FIGURE 13

RF and FSO attenuations exceeded for different time percentages

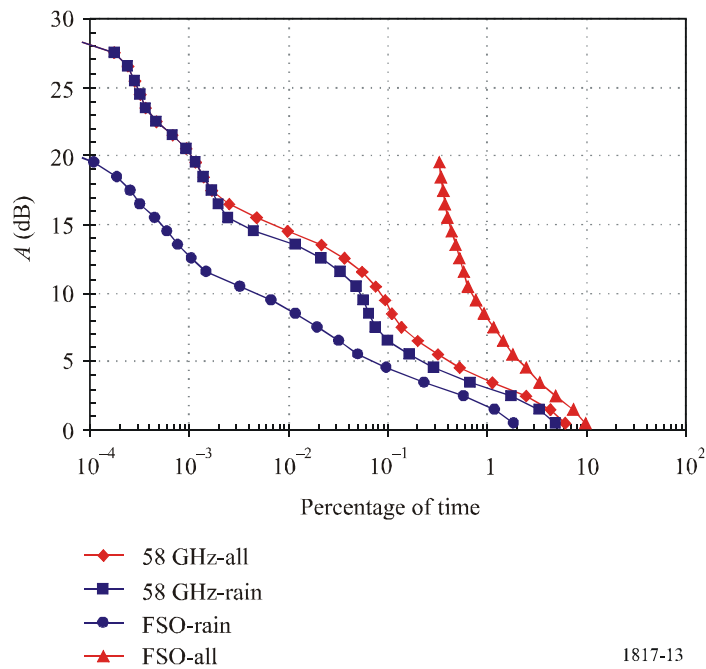


TABLE 3

**Availability ratio comparison of RF, FSO and
hypothetical RF/FSO hybrid systems**

System	AR (%)
FSO part (850 nm)	99.7
RF part (58 GHz)	99.999
Hybrid RF/FSO	99.9999

12 Visibility measurement

The visibility V (km) is defined as the distance to an object where the image contrast drops to 2% of its original value. It is measured at 550 nm, the wavelength that corresponds to the maximum intensity of the solar spectrum, and is given by the Koschmieder relation:

$$V(\text{km}) = \frac{3.912}{\gamma_{550 \text{ nm}}} \quad (12)$$

where $\gamma_{550 \text{ nm}}$ is the extinction coefficient of the medium (atmosphere and aerosols).

Two types of sensors are used to measure the visibility: transmissometers and diffusimeters.

The international visibility code showing the attenuation (dB/km) for various climatic conditions is shown in the following table:

- Weather conditions from very clear periods to dense fog.
- Precipitation (mm/h): drizzle, rain, storm.
- Visibility from 50 m to 50 km.

International visibility code				
Weather conditions	Precipitation		Visibility (m)	Attenuation (dB/km)
		mm/h		
Dense fog			0	
Thick fog			50	315
Moderate fog			200	75
Light fog			500	28.9
Very light fog	Storm	100	770	18.3
			1 000	13.8
Light mist	Strong rain	25	1 900	6.9
			2 000	6.6
Very light mist	Average rain	12.5	2 800	4.6
			4 000	3.1
Clear air	Light rain	2.5	5 900	2
			10 000	1.1
Very clear air	Drizzle	0.25	18 100	0.6
			20 000	0.54
			23 000	0.47
			50 000	0.19

Appendix 1 to Annex 1

Computer modelling

From the theoretical description of the physical phenomena, a certain number of computer modelling programs have been developed to determine the atmospheric transmission coefficient. Several models are available: LOWTRAN and NAM programs (Navy Aerosol Model); NOVAM and WKDAER in maritime environments, etc. NOVAM is included in MODTRAN, FASCOD, etc.

LOWTRAN contains models of optical signal attenuation by aerosols. It is based on a line-by-line model and is available from ONTAR (United States of America).

NAM software applies more particularly to maritime environments. It is based on the aerosol distribution model of GATHMAN.

NOVAM takes into account dust particles of continental origin.

WKDAER can be adjusted to a specific environment.

FASCOD uses a line-by-line model and takes into account all parameters characterizing the absorption lines (intensity, transition probability, etc.). It is based on the high-resolution molecular absorption database, HITRAN. The principal line parameters included in HITRAN are the resonance frequency, line intensity at 296 K, probability of a transition, half-width of the line at 296 K, and the low energy or fundamental molecular state.

There are three linked models developed in the Air Force Geophysics Laboratory (AFGDL) with various spectral resolutions:

- LOWTRAN 7 – Low Resolution Transmission – Spectral resolution is 20 cm^{-1} (equivalent to 600 GHz) in 5 cm^{-1} steps.
- MODTRAN 3 – Moderate Resolution Transmission – Spectral resolution is 2 cm^{-1} (equivalent to 60 GHz) in 1 cm^{-1} steps.
- HITRAN 2004 – High Resolution Transmission – Spectral resolution is 0.001 cm^{-1} (equivalent to 30 MHz).

All of the models contain spectral information about many atmospheric species including H_2O , O_3 , N_2O , CO , CH_4 , O_2 , NO , NO_2 , SO_2 , and HNO_3 . (HITRAN includes details of over 1 000 000 absorption lines for 37 molecules.) In addition the three models include the H_2O continuum across the entire spectrum, the N_2 continuum in the 2 000 to 2 700 cm^{-1} region, molecular scattering, together with absorption and scattering from aerosol, fog, rain and clouds.
